Chemical Engineering Research and Design 204 (2024) 121–136

Contents lists available at ScienceDirect

Chemical Engineering Research and Design

journal homepage: www.elsevier.com/locate/cherd

Optimal hydrogen infrastructure planning for heat decarbonisation

Margarita E. Efthymiadou, Vassilis M. Charitopoulos, Lazaros G. Papageorgiou *

The Sargent Centre for Process Systems Engineering, Department of Chemical Engineering, University College London (UCL), Torrington Place, London WC1E 7JE, UK

ARTICLE INFO

Keywords:
Energy systems modelling
Hydrogen infrastructure
Mixed integer linear programming
What-if analysis
Heat decarbonisation
Net-Zero

ABSTRACT

Energy decarbonisation is essential to achieve Net-Zero emissions goal by 2050. Consequently, investments in alternative low-carbon pathways and energy carriers for the heat sector are required. In this study, we propose an optimisation framework for the transition of heat sector in Great Britain focusing on hydrogen infrastructure decisions. A spatially-explicit mixed-integer linear programming (MILP) evolution model is developed to minimise the total system's cost considering investment and operational decisions. The optimisation framework incorporates both long-term planning horizon of 5-year steps from 2035 to 2050 and typical days with hourly resolution. Aiming to alleviate the computational effort of such multiscale model, two hierarchical solution approaches are suggested that result in computational time reduction. From the optimisation results, it is shown that the installation of gas reforming hydrogen production technologies with CCS and biomass gasification with CCS can provide a cost-effective strategy achieving decarbonisation goal. What-if analysis is conducted to demonstrate further insights for future hydrogen infrastructure investments. Results indicate that, as cost is highly dependent on natural gas price, Water Electrolysis capacity increases significantly when gas price rises. Moreover, the introduction of carbon tax policy can lead to lower CO_2 net emissions.

1. Introduction

1.1. Motivation

In the last decades, global greenhouse gas emissions have increased rapidly resulting in a significant rise of global temperature by almost 1 °C from mid-1970 (BEIS, 2022). In order to hedge against climate change, the UK has set a goal to achieve Net-Zero target by 2050, while reducing emissions by approximately 78% by 2035 in comparison with 1990 emissions levels (CCC, 2020). In this context, a strategy has been published by HM Government (2021) and International Energy Agency (IEA, 2021) describing alternative pathways to achieve Net-Zero goal.

The energy sector is responsible for about three quarters of global greenhouse gas emissions today (IEA, 2021) due to fossil fuels, which are widely used for energy production. Thus, energy systems decarbonisation is inevitable and the use of “green fuels” in the form of electricity, hydrogen, ammonia or synthetic hydrocarbons is required. According to national statistics, 16% of the UK greenhouse gas emissions are estimated to come from residential sector (BEIS, 2023). Therefore, an increasing attention for the role of hydrogen in the decarbonisation of heat has emerged in the last years (BEIS, 2018).

As energy transition is a highly complex challenge for the industrialised societies, many governments around the world have started funding researches and projects launching plans of hydrogen as a future fuel. The UK has a leadership role in tackling climate change and taking measures to end its contribution in global warming. To this end, Department for Business, Energy & Industrial Strategy (BEIS, 2021c) published its UK Hydrogen Strategy policy paper suggesting that hydrogen demand will increase significantly in the following years and the installed production capacity of hydrogen will reach up to 20 GW by 2035.

Hydrogen is a key element in meeting Net-Zero target either as an alternative for natural gas or as an energy carrier of renewable electricity generation. Towards heat sector decarbonisation, hydrogen can play an important role in the energy mix. Studies focus on the direct use of hydrogen in heat appliances either as a mix with natural gas or as pure hydrogen.

Regarding the direct use of hydrogen, changes in heating appliances and pipework in the building are necessary. However, safety issues may arise from these changes (Element Energy and E4tech, 2018). Thus, risk reduction measures are suggested to safely install hydrogen infrastructure (Hy4Heat and BEIS, 2021). These measures include frequent maintenance, appropriate ventilation, internal pipework refinement, hydrogen detection alarms and awareness of residents.

* Corresponding author.
E-mail address: l.papageorgiou@ucl.ac.uk (L.G. Papageorgiou).

https://doi.org/10.1016/j.cherd.2024.02.028
Received 23 November 2023; Received in revised form 13 February 2024; Accepted 14 February 2024
Available online 19 February 2024
0263-8762/

Consequently, as new hydrogen infrastructure networks connecting supply to demand are required, a novel modelling tool for hydrogen supply chain is essential to investigate design decisions. This work focuses on the hydrogen production, storage and transmission infrastructure to meet the heat demand in Great Britain.

1.2. Literature review

Optimisation in hydrogen infrastructure planning is a field receiving considerable attention in the PSE community in the last decades. One of the first integrated framework for hydrogen supply chains design and operation using mathematical modelling approach was developed by Hugo et al. (2005). The authors proposed a MILP evolution model for the strategic investment decisions of future hydrogen infrastructure for supplying hydrogen fuel cell vehicles. In this work, the decisions for optimal infrastructure are based on both economic and environmental criteria. Almansoori and Shah (2006) introduced a MILP snapshot spatially-explicit model determining the optimal infrastructure strategy to meet hydrogen demand in transport sector in the UK. Then, they extended their model taking into account the evolution of demand over the time horizon (Almansoori and Shah, 2009).

In the last decade, considerable literature has addressed hydrogen supply chain infrastructure design to meet hydrogen demand for transportation sector using different multi-objective optimisation approaches. A bi-criterion model for simultaneous minimisation of system cost and environmental impact of the system was proposed by Guillén-Gosálbez et al. (2010). The greenhouse gas emissions of this study considered the entire life cycle of the process. Almaraz et al. (2013) have introduced a snapshot model using multi-objective optimisation taking into account cost, environmental impact and safety risk of hydrogen infrastructure for transportation demand in Great Britain. The aforementioned group extended their model into a multi-period spatial model in two case studies. The first case study focused on the hydrogen transportation demand in mainland France (Almaraz et al., 2014) while the second work used a case study on mobility and industry hydrogen demand in Hungary (Almaraz et al., 2022).

Agnolucci et al. (2013) proposed a spatially-explicit multi-period MILP model (SHIPmod), which was applied in different scenarios for meeting hydrogen transport demand in the UK. This study was the first, to the best of author's knowledge, that included a carbon capture and storage system (CCS) in Hydrogen Supply Chain (HSC) model. The CCS system consisted of CO_2 pipeline network and reservoirs for CO_2 emissions in the pathway of low-carbon hydrogen production. Moreover, a hierarchical procedure was proposed for decreasing the computational time for solving of large-scale problems. Next, Moreno-Benito et al. (2017) extended the SHIPmod formulation by adding hydrogen pipelines for regional transmission and local distribution. The authors concluded that steam methane reforming coupled with carbon capture and storage is the most economical low-carbon production technology. Hydraulics of hydrogen pipelines were investigated by Weber and Papageorgiou (2018). They created a multi-objective MILP formulation minimising the total system cost and the risk of a hydrogen pipeline operation.

Ogumerem et al. (2018) developed a multi objective spatially-explicit multi period MILP model of hydrogen network for transportation demand using a case study in Texas. In this work, the role of oxygen as a by-product from water electrolysis was studied. The authors investigated two cases: oxygen as a discarded or revenue generating by-product. They concluded that hydrogen from electrolysis apart from being a low-carbon technology, can be an economically viable option when oxygen is treated as revenue generating by-product.

One of the first works that simultaneously determined the design and operation of a hydrogen network in hourly resolution was STeMES (Samsatli et al., 2016). STeMES is an integrated wind, hydrogen and electricity model with spatial resolution aiming at decarbonising the transportation sector in Great Britain. He et al. (2021) proposed a snapshot spatial model which determines the least-cost hydrogen planning for multiple end-uses in the US Northeast. The framework included production unit commitment and flexible scheduling for hydrogen transmission. Their results suggested that trucks used as both transmission and storage can provide significant extra flexibility to the system and decrease the total system cost.

In the recent years, there is a growing interest in the decarbonisation of heating sector using low-carbon hydrogen. Samsatli and Samsatli (2019) have developed a spatio-temporal MILP model (Value Web Model) to investigate the role of hydrogen from renewable electricity in decarbonising heat. Their results showed that hydrogen storage is an important part of the network profitability. An MILP framework, which took into account production technologies with CCS and electrolysis, for the design of a hydrogen based heating system was proposed by Sunny et al. (2020). The authors concluded that auto-thermal reforming is the most cost effective technology for CO_2 mitigation.

Seo et al. (2020) introduced a spatial hydrogen supply chain model from supplier to end-use with centralised storage. From their case study in Korea, they concluded that centralised storage could reduce levelised hydrogen cost compared with decentralised storage. Green hydrogen as shipping fuel was studied by Kazi and Eljack (2022). Their work focuses on green hydrogen economy in both industry and maritime sector in Qatar. More specifically, they developed a spatio-temporal MILP model with one year time steps until 2030. The multi-objective optimisation aimed at the reduction of both system cost and the greenhouse gas emissions.

1.3. Contribution of this work

The proposed framework investigates the expansion planning of hydrogen infrastructure to meet residential heat demand in the UK. Hourly resolution is considered to deal with demand and renewables availability fluctuations during the day. The optimisation framework includes CCS investment decisions which are required for a long-term low-carbon hydrogen infrastructure planning. Furthermore, in the context of green hydrogen production from water electrolysis, the electricity generation from renewable sources is considered in this model.

The spatio-temporal resolution and the number of technologies result in a model of high combinatorial complexity which can be decreased using solution procedures. To this end, the large-scale model can be divided into smaller models which are easier to solve without compromising the quality of the solution. Therefore, two hierarchical approaches have been developed for computational time reduction, which allows us to add more features to the model and increase spatio-temporal resolution.

To provide a more comprehensive view of the hydrogen based system, a what-if analysis has been conducted regarding gas price, carbon tax and biomass availability. From the optimisation of different cases, environmental and economic insights can be obtained for the conversion to a hydrogen based heating system.

Conclusively, the novelty of this work focuses on:

- the development of a multi-scale optimisation framework, and
- the introduction of two hierarchical approaches to enhance computational efficiency.

The remainder of the paper is structured as follows: The problem statement is described in Sections 2 and 3 details the mathematical model. A description of solution procedures is presented in Section 4. A case study on hydrogen infrastructure planning for heat decarbonisation in Great Britain is described in Section 5. Section 6 focuses on the results and what-if analysis discussion. Finally, the concluding remarks are summarised in Section 7.

2. Problem statement

The goal of this work is the optimal design of hydrogen infrastructure over a planning horizon to meet the hydrogen residential heating demand while satisfying the Greenhouse Gas (GHG) Net-Zero emission targets. The proposed Supply Chain (SC) model includes design decisions concerning the location, the type and the capacity of production and storage investments, the size and the location of hydrogen and CO_2 pipelines and the commission of CO_2 reservoirs. Moreover, it aims to determine production, storage and transmission decisions on typical days. The optimisation problem is stated as follows.

Given:

- Hydrogen heating demand and renewables availability in each region, time period, cluster and hour;
- Capital and operating costs for hydrogen production technologies, hydrogen storage sites, renewables farms, hydrogen and CO_2 pipelines;
- Minimum and maximum capacity and ramp rates as well as the lifetime of production plants and storage sites;
- Minimum and maximum flowrate in pipelines;
- Capacity of hydrogen caverns and CO_2 reservoirs;
- Hydrogen import price;
- Carbon tax and capture rates for CO_2 emissions as well as CO_2 emission targets for each year;
- Land availability and biomass availability.

To determine the optimal:

- Location and capacity of production technologies and storage sites;
- Hydrogen production and storage rate in each region, time period, representative day and hour;
- Hydrogen and CO_2 transmission investments between regions;
- Hydrogen and CO_2 flowrates between regions in each time period, representative day and hour;
- Electricity generation of renewables in each region, time period, representative day and hour;
- Hydrogen import rates in each time period, representative day and hour.

So as to minimise the total system cost subject to GHG emission targets.

The key assumptions for this work are summarised as follows:

- Gas hourly demand profiles (Charitopoulos et al., 2023) are used as a proxy for gas consumption which is required for residential heating;
- A gas price prediction is used for the 5-year period according to Future Energy Scenarios (National Grid ESO, 2022);
- Hydrogen transmission between regions takes place through pipelines;
- Transmission distances are calculated as the distance between centroids of each region;
- Hydrogen pipeline connections are designed according to the connections of the incumbent gas pipeline network;
- Hydrogen distribution within a region is not modelled;
- Water Electrolysis production units use electricity generated from renewable farms;
- Variable operating cost for renewable farms is assumed zero;
- Curtailment cost is not taken into account.

3. Mathematical model

3.1. Spatio-temporal resolution

The temporal resolution (illustrated in Fig. 1) of the hydrogen system is dual to incorporate both design and operating decisions. The hydrogen system transition is studied from 2035 to 2050 using 5-year steps to define the optimal design decisions. On the other hand, in each 5-year time step, typical days are studied for operating decisions, such as production and storage rates. On a daily basis, hourly resolution is employed to consider peak-hour demand as well as the fluctuations in the availability of solar, wind onshore and wind offshore technologies.

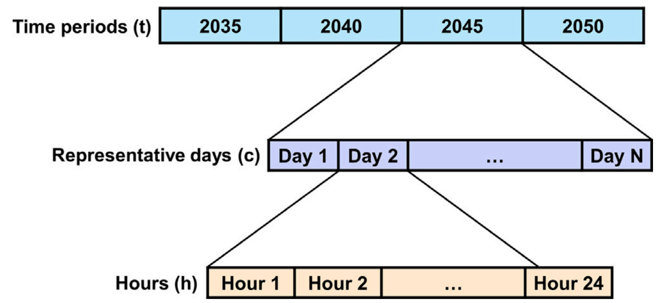

Fig. 1. Multi-scale temporal resolution.

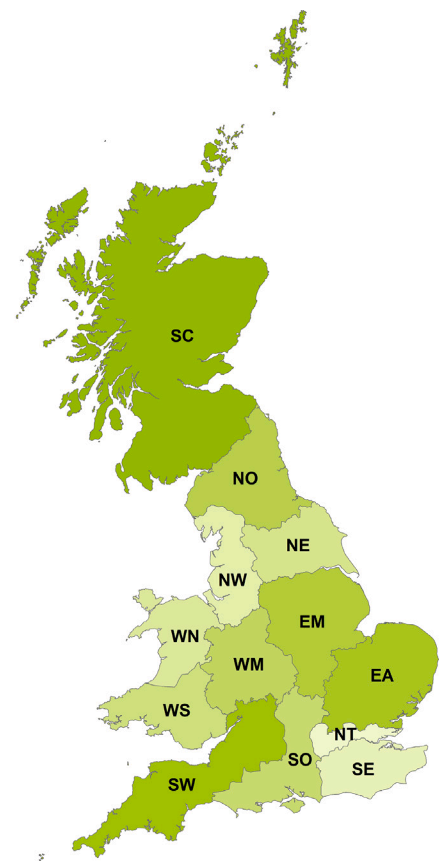

Fig. 2. Regional representation of Great Britain.

K-medoids clustering is used for representative days selection. More specifically, the days that share similar hourly profiles for heat demand, wind and solar availability are agglomerated in the same representative day (cluster). K-medoids clustering method is used as the real days can produce more accurate results incorporating higher variations than an average profile (Kotzur et al., 2018). Furthermore, Great Britain is divided in 13 regions according to local gas Distribution Zones (LDZ) of the incumbent natural gas network, as illustrated in Fig. 2.

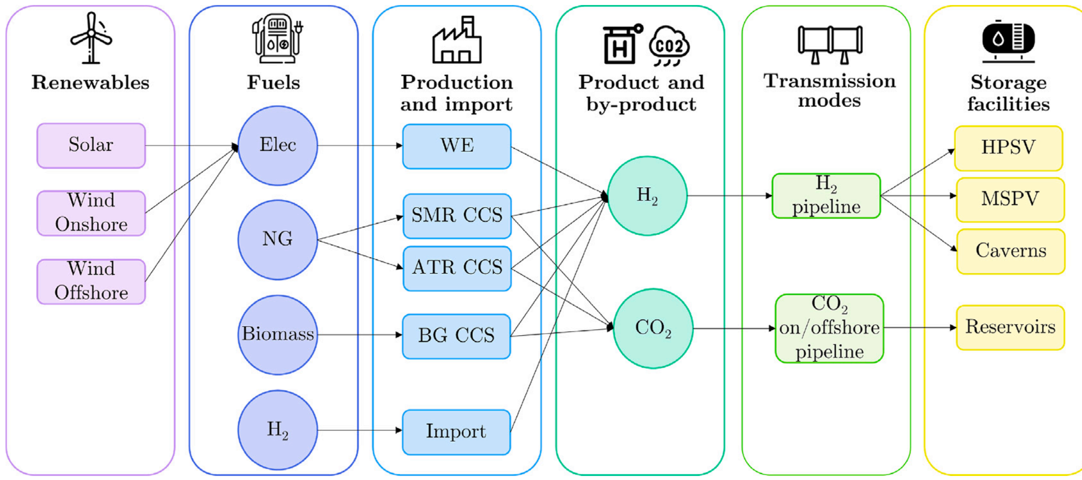

Fig. 3. Hydrogen and CO_2 infrastructure.

3.2. Superstructure

This case study includes hydrogen production, storage and transmission technologies and a carbon capture and storage (CCS) system as illustrated in Fig. 3.

The technologies which are considered in the H_2 model for hydrogen production are Steam Methane Reforming (SMR) with Carbon Capture and Storage (CCS), Auto-thermal Reforming (ATR) with CCS, Biomass Gasification (BG) with CCS and Water Electrolysis (WE).

The aforementioned technologies are coupled with a CCS system to decrease GHG emissions in the context of reducing the environmental footprint in hydrogen production to achieve heat decarbonisation. CO_2 produced from the chemical reactions can be captured using an amine solvent. Amine CO_2 removal systems constitute mature technologies (Walker et al., 2018) and work in an absorber-regeneration loop (Liang et al., 2015).

Moreover, for water electrolysis, PEM (Polymer electrolyte membrane) technology is considered as it offers high operating density and smaller environmental footprint (Kumar and Lim, 2022). It is worth mentioning that the electricity required for WE is generated from renewable technologies. Solar panels, Wind Onshore and Wind Offshore farms are taken into account in this case study.

Hydrogen storage is a key element in hydrogen economy to address the future high demands and the demand peaks. In this study, two types of storage vessels, High Pressure Storage Vessel (HPSV) and Medium Pressure Storage Vessel (MSPV), are considered. Hydrogen can be transmitted between regions through pipelines. The neighbouring connections which are allowed three discrete alternatives for pipeline diameters are considered (0.5 m, 0.8 m and 1 m).

To meet Net-Zero goal, CCS system is included in the system infrastructure. CO_2 emissions are captured from the production units and they are transmitted to the CO_2 reservoirs through pipelines. Two diameters alternative are considered in this case study (0.6 m and 1.2 m). Moreover, the CO_2 reservoirs which are taken into consideration in this study, are located in North and Irish Sea.

The detailed techno-economical data for the model were collected from different sources and they can be found in the Supplementary Information.

3.3. Mathematical framework

The mathematical model presented in this Section is an extension of the multi-period spatially explicit mathematical framework (SHIPmod) developed by Agnolucci et al. (2013) and Moreno-Benito et al. (2017). The aforementioned framework is extended to include renewable technologies for electricity generation used as feedstock for water electrolysis. Moreover, in the proposed model, key constraints for long term low-carbon hydrogen transition such as emission targets, land and biomass availability are considered. Another focal extension is the introduction of hourly temporal resolution to incorporate hourly fluctuations in demand and production rates.

3.3.1. Objective function

Total Cost

The model's objective function is the minimisation of the total system cost. The total cost (TC) consists of the production capital cost (PCC), the storage capital cost (SCC), the transportation capital cost (TCC), the production operational cost (POC), the storage operational cost (SOC), the transportation operational cost (TOC), the carbon emissions cost (CEC), the hydrogen import costs (IIC) and the renewables cost (ReC).

$$TC = PCC + SCC + PLCC + POC + SOC + PLOC + CEC + IIC + ReC \\ + BC + NGC \tag{1}$$

Production Costs

The production capital cost (PCC) depends on the number of the new hydrogen plant investments (IP_{pgt}) which are installed in each region g and each time period t, while production operational cost (POC) depends on the number of the available hydrogen plants (NP_{pgt}) and the production rate (Pr_{pgtch}) in each production type p, region g, time period t, cluster c and hour h.

$$PCC = \sum_{p\in P}\sum_{g\in G}\sum_{t\in T} dfc_t \cdot pcc_{pt} \cdot cap_p^P \cdot IP_{pgt} \tag{2}$$

$$POC = \sum_{p\in P}\sum_{g\in G}\sum_{t\in T} dfo_t \left[poc_{pt}^F \cdot cap_p^P \cdot NP_{pgt} + \sum_{c\in C}\sum_{h\in H} WF_c \cdot poc_{pt}^V \cdot Pr_{pgcht} \right] \tag{3}$$

where n the duration of the time period while dfc_t and dfo_t are the discount factors for capital and operational costs, respectively, and are calculated in Supplementary Information. pcc_{pt}, poc_{pt}^F, poc_{pt}^V stand for the capital, fixed operational and variable operational cost of hydrogen production for production type p and time period t and cap_p^P stands for the production capacity of production technology p. WF_c is the weight of days for each typical day (cluster) c.

Storage Costs

The storage capital cost (SCC) depends on the number of the new hydrogen storage investments (IS_{sgt}) which are installed in each region g and each time period t while storage operational cost (SOC) depends on the number of the available storage sites s and the storage level (St_{sgtch}) in each storage type s, region g, time period t, cluster c and hour h.

$$SCC = \sum_{s \in S} \sum_{g \in G} \sum_{t \in T} dfc_t \cdot scc_{st} \cdot cap_s^S \cdot IS_{sgt} \tag{4}$$

$$SOC = \sum_{s \in S} \sum_{g \in G} \sum_{t \in T} dfo_t \left[soc_{st}^F \cdot cap_s^S \cdot NS_{sgt} + \sum_{c \in C} \sum_{h \in H} WF_c \cdot soc_s^V \cdot St_{sgcht} \right] \tag{5}$$

where dfc_t and dfo_t are the discount factors for capital and operational costs respectively while n the duration of the time period. scc_{st}, soc_{st}^F, soc_s^V stand for the capital, fixed operational and variable operational cost of hydrogen storage for storage site s and time period t and $SCap_s$ stands for the storage capacity.

Transportation Costs

Hydrogen can be transported through pipelines. The total pipeline cost consists of the pipeline capital cost ($PLCC$) and the pipeline operating cost ($PLOC$).

The pipeline capital cost ($PLCC$) consists of hydrogen pipeline cost between regions and to storage caverns, CO_2 onshore pipeline cost and CO_2 offshore pipeline cost to reservoirs. The pipeline operating cost ($PLOC$) is assumed to be a certain fraction of the pipeline capital cost (δ, $\overline{\delta}$, $\overline{\overline{\delta}}$).

$$\begin{aligned} PLCC = & \sum_{d \in D} \sum_{t \in T} \sum_{g,g' \in N_{gg'}^{pipe}} dfc_t \cdot pc_d \cdot D_{gg'}^{pipe} \cdot Y_{dgg't} \\ & + \sum_{d \in D} \sum_{t \in T} \sum_{g,s \in GS_{gs}} dfc_t \cdot pc_d \cdot D_{gs}^{st} \cdot Y_{dgst}^S \\ & + \sum_{d \in D} \sum_{t \in T} \sum_{g,g' \in N_{gg'}} dfc_t \cdot \overline{pc}_d \cdot D_{gg'}^{pipe} \cdot \overline{Y}_{dgg't} \\ & + \sum_{d \in D} \sum_{t \in T} \sum_{g,r \in GR_{gr}} dfc_t \cdot \overline{\overline{pc}}_d \cdot D_{gg'}^{res} \cdot \overline{\overline{Y}}_{dgrt} \end{aligned} \tag{6}$$

$$\begin{aligned} PLOC = & \sum_{d \in D} \sum_{t \in T} \sum_{g,g' \in N_{gg'}^{pipe}} \delta \cdot dfo_t \cdot crf \cdot pc_d \cdot D_{gg'}^{pipe} \cdot AY_{dgg't} \\ & + \sum_{d \in D} \sum_{t \in T} \sum_{g,s \in GS_{gs}} \delta \cdot dfo_t \cdot crf \cdot pc_d \cdot D_{gs}^{st} \cdot AY_{dgst}^S \\ & + \sum_{d \in D} \sum_{t \in T} \sum_{g,g' \in N_{gg'}} \overline{\delta} \cdot dfo_t \cdot crf \cdot \overline{pc}_d \cdot D_{gg'}^{pipe} \cdot \overline{AY}_{dgg't} \\ & + \sum_{d \in D} \sum_{t \in T} \sum_{g,r \in GR_{gr}} \overline{\overline{\delta}} \cdot dfo_t \cdot crf \cdot \overline{\overline{pc}}_d \cdot D_{gg'}^{res} \cdot \overline{\overline{AY}}_{dgrt} \end{aligned} \tag{7}$$

where $Y_{dgg't}$, $AY_{dgg't}$, Y_{dgst}^S, AY_{dgst}^S, $\overline{Y}_{dgg't}$, $\overline{AY}_{dgg't}$, $\overline{\overline{Y}}_{dgrt}$ and $\overline{\overline{AY}}_{dgrt}$ stand for the new pipeline investment and the available pipelines for regional hydrogen transmission, storage hydrogen transmission, onshore and offshore CO_2 transmission, respectively. $D_{gg'}^{pipe}$ is the distance between two regions through pipeline, D_{gs}^{st} is the distance between a region g and the underground storage s and $D_{gg'}^{res}$ is the distance between the region g and the CO_2 reservoir r. pc_d, $\overline{pc}_d$ and $\overline{\overline{pc}}_d$ are the pipeline cost for each diameter d, while crf is the capital recovery factor.

Renewables Cost

The renewables cost (ReC) depends on the new installed capacity (IR_{egt}) and the available capacity (NR_{egt}) of renewable e in region g and time period t. It is calculated as in Eq. (8).

$$ReC = \sum_{e \in E} \sum_{g \in G} \sum_{t \in T} (dfc_t \cdot rc_{et} \cdot IR_{egt} + dfo_t \cdot ro_{et} \cdot NR_{egt}) \tag{8}$$

where rc_{et} and ro_{et} are the renewable capital and operating cost, respectively, for renewable e and time period t.

Carbon Emissions Cost

The emissions cost depends on the carbon emissions cost (ct_t) for each time period t and the total CO_2 emissions, which results from the hydrogen production rate (Pr_{pgtch}) multiplied with the coefficient of CO_2 emissions (ye_{pt}) for each production technology and time period.

$$CEC = \sum_{p \in P} \sum_{g \in G} \sum_{t \in T} \sum_{c \in C} \sum_{h \in H} WF_c \cdot dfo_t \cdot ct_t \cdot ye_{pt} \cdot Pr_{pgtch} \tag{9}$$

Import Cost

The import cost is computed based on the import price (p^{imp}) and the import rate (Imp_{gtch}).

$$IIC = \sum_{g \in GI} \sum_{t \in T} \sum_{c \in C} \sum_{h \in H} WF_c \cdot dfo_t \cdot p^{imp} \cdot Imp_{gtch} \tag{10}$$

where GI is the set which denotes the regions that hydrogen can be imported.

Fuels Cost

The cost of the natural gas used in the reforming technologies can be calculated from Eq. (11).

$$NGC = \sum_{t \in T} dfo_t \cdot c_t^{gas} \cdot V_t^{gas} \tag{11}$$

where c_t^{gas} stands for the gas price and V_t^{gas} stands for the gas consumption.

Similarly, the cost of biomass which is used for biomass gasification can be estimated from Eq. (12).

$$BC = \sum_{g \in G} \sum_{t \in T} dfo_t \cdot c_t^{bio} \cdot V_{gt}^{bio} \tag{12}$$

where c_t^{bio} stands for the biomass price and V_t^{bio} stands for the biomass consumption.

3.3.2. Mass and energy balances

Hydrogen energy balance and CO_2 mass balance are depicted in Fig. 4. Hydrogen energy balance can be described by Eq. (13). More specifically, in each region g, time period t, cluster c and hour h, the total production rate (Pr_{pgtch}), the flowrates ($Q_{g'gtch}$) to region g, the rejected hydrogen from storage site s and the imported hydrogen (Imp_{gtch}) are equal to the flowrates ($Q_{gg'tch}$) from region g, the injected hydrogen to storage sites s (Q_{gstch}^I) and the total demand (TD_{gtch}).

$$\begin{aligned} & \sum_{p \in P} Pr_{pgtch} + \sum_{l \in \{Pipe\}} \sum_{g' \in N_{g'g}^{pipe}} Q_{g'gtch} + \sum_{s \in GS_{gs}} Q_{gstch}^R + Imp_{gtch} \\ & \quad = \sum_{l \in \{Pipe\}} \sum_{g' \in N_{gg'}^{pipe}} Q_{gg'tch} + \sum_{s \in GS_{gs}} Q_{gstch}^I + TD_{gtch} \\ & \quad \forall g \in G, t \in T, c \in C, h \in H \end{aligned} \tag{13}$$

The CO_2 mass balance can be expressed by Eq. (14). The left-hand side represents the onshore CO_2 flowrates to region g from other regions g' ($\overline{Q}_{g'gtch}$) and the captured CO_2, which is equal to the hydrogen production rate (Pr_{pgtch}) multiplied by a coefficient of CO_2 capture for each production technology type (y_{pt}^c). The right-hand side represents the onshore CO_2 flowrates from region g to other regions g' ($\overline{Q}_{gg'tch}$) and the offshore CO_2 flowrates ($\overline{\overline{Q}}_{grtch}$) from region g to reservoir r.

$$\begin{aligned} & \sum_{g' \in N_{g'g}} \overline{Q}_{g'gtch} + \sum_{p} y_{pt}^c Pr_{pgtch} = \sum_{g' \in N_{gg'}} \overline{Q}_{gg'tch} + \sum_{r \in GR_{gr}} \overline{\overline{Q}}_{grtch} \\ & \quad \forall g \in G, t \in T, c \in C, h \in H \end{aligned} \tag{14}$$

3.3.3. H_2 production

The hydrogen production rate is limited by an upper and lower bound according to Eq. (15).

$$cap_p^{min} \cdot NP_{pgt} \le Pr_{pgtch} \le cap_p^{max} \cdot NP_{pgt}$$

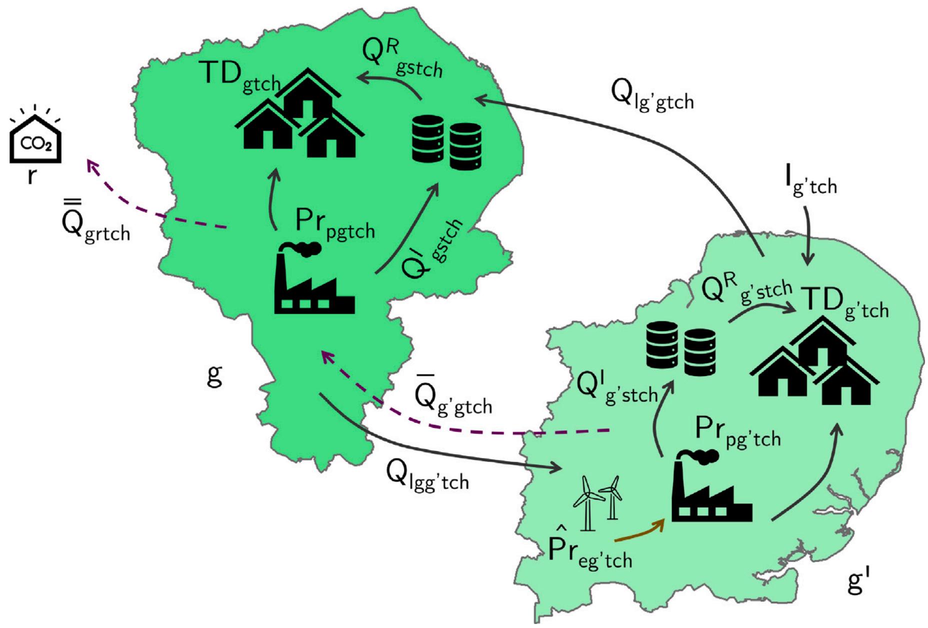

Fig. 4. Visual representation of energy and mass balance for regions g and g'.

$$\forall p \in P, g \in G, t \in T, c \in C, h \in H \tag{15}$$

where cap^{min}_p and cap^{max}_p are the minimum and maximum capacity of a production plant while NP_{pgt} is the number of available production plant of technology p, region g and time period t.

The production plants availability is defined by Eq. (16).

$$NP_{pgt} = NP_{pg,t-1} + IP_{pgt} - IP_{pg,t-(\frac{LT^P_p}{n})} \qquad \forall p \in P, g \in G, t \in T \tag{16}$$

where IP_{pgt} is the new invested production plants and LT^P_p is the lifetime of production technology p.

The operation of production plants is restricted by their hourly ramp-up and ramp-down capabilities.

$$Pr_{pgtch} - Pr_{pgtc,h-1} \le RU_p \cdot cap^P_p \cdot NP_{pgt}$$
$$\forall p \in P, g \in G, t \in T, c \in C, h > 1 \tag{17}$$

$$Pr_{pgtc,h-1} - Pr_{pgtch} \le RD_p \cdot cap^P_p \cdot NP_{pgt}$$
$$\forall p \in P, g \in G, t \in T, c \in C, h > 1 \tag{18}$$

where RU_p and RD_p are the ramp up and down rates for each production technology type p.

3.3.4. H_2 storage

Storage rate is limited by an upper and lower bound as defined in Eq. (19).

$$cap^{Smin}_s \cdot NS_{sgt} \le St_{sgtch} \le cap^{Smax}_s \cdot NS_{sgt}$$
$$\forall \{s,g\} \in GS_{gs}, t \in T, c \in C, h \in H \tag{19}$$

where cap^{min}_s and cap^{max}_p are the minimum and maximum storage rate while NS_{sgt} is the number of available storage sites of technology s, region g and time period t.

The storage site availability is defined by Eq. (20):

$$NS_{sgt} = NS_{sg,t-1} + IS_{sgt} - IP_{sg,t-(\frac{LTs_s}{a})} \qquad \forall \{s,g\} \in GS_{gs}, t \in T \tag{20}$$

where IS_{sgt} is the new invested storage sites and LTs_s is the lifetime of storage technology s.

The storage rate (St_{sgtch}) is equal to the storage rate in the previous hour and the hydrogen which is injected minus the hydrogen which is rejected in each storage site s, region g, time period t, cluster c and hour h. St^{init} is the initial storage rate in the first hour. Moreover, the storage rate in last hour is equal to the initial storage rate of the daily horizon according to Eq. (22). The aforementioned equation is incorporated to ensure the interconnectedness of the storage level between the days.

$$St_{sgtch} = St^{init}|_{h=1} + St_{sgtc,h-1} + Q^I_{gstch} - Q^R_{sgtch}$$
$$\forall \{s,g\} \in GS_{gs}, t \in T, c \in C, h \in H \tag{21}$$

$$St_{sgtc,24} = St^{init} \qquad \forall \{s,g\} \in GS_{gs}, t \in T, c \in C \tag{22}$$

Moreover, upper bounds are imposed for the injection and removal rate.

$$Q^I_{gstch} \le Q^{Imax}_s \cdot NS_{sgt} \qquad \forall \{s,g\} \in GS_{gs}, t \in T, c \in C, h \in H \tag{23}$$

$$Q^R_{gstch} \le Q^{Rmax}_s \cdot NS_{sgt} \qquad \forall \{s,g\} \in GS_{gs}, t \in T, c \in C, h \in H \tag{24}$$

where Q^{Imax}_s and Q^{Rmax}_s are the maximum injection and rejection rate for each storage type s.

3.3.5. H_2 and CO_2 pipeline

The maximum flowrate in the pipelines can be described by Eqs. (25)–(27) for the hydrogen flowrate ($Q_{gg'tch}$), onshore CO_2 flowrate ($\overline{Q}_{gg'tch}$) and offshore CO_2 flowrate ($\overline{\overline{Q}}_{grtch}$).

$$Q_{gg'tch} \le \begin{cases} \sum_{d \in D} q^{Hmax}_d \cdot AY_{dgg't} & \forall g < g' \in N^{pipe}_{gg'}, t \in T, c \in C, h \in H \\ \sum_{d \in D} q^{Hmax}_d \cdot AY_{dg'gt} & \forall g' < g \in N^{pipe}_{gg'}, t \in T, c \in C, h \in H \end{cases} \tag{25}$$

$$\overline{Q}_{gg'tch} \le \begin{cases} \sum_{d \in D} q^{Cmax}_d \cdot \overline{AY}_{dgg't} & \forall g < g' \in N_{gg'}, t \in T, c \in C, h \in H \\ \sum_{d \in D} q^{Cmax}_d \cdot \overline{AY}_{dg'gt} & \forall g' < g \in N_{gg'}, t \in T, c \in C, h \in H \end{cases} \tag{26}$$

$$\overline{\overline{Q}}_{grtch} \le \sum_{d \in D} q^{Cmax}_d \cdot \overline{\overline{AY}}_{dgrt} \qquad \forall \{g,r\} \in GR_{gr}, t \in T, c \in C, h \in H \tag{27}$$

where q^{Hmax}_d and q^{Cmax}_d are the maximum flowrate for each diameter size d for hydrogen and CO_2, respectively.

Pipeline availability for hydrogen transmission between regions and to the storage caverns and for onshore and offshore CO_2 transmission are defined by Eqs. (28)–(31).

$$AY_{dgg't} = AY_{dgg',t-1} + Y_{dgg't} - Y_{dgg',t-(\frac{LT^{pipe}}{n})} \quad \forall\{g,g'\} \in N^{pipe}_{gg'}, d \in D, t \in T, g < g' \tag{28}$$

$$AY^S_{d\,g\,sc\,t} = AY^S_{d\,g\,sc,t-1} + Y^S_{d\,g\,sc\,t} - Y^S_{d\,g\,sc,t-(\frac{LT^{pipe}}{n})} \quad \forall\{g,sc\} \in GS_{g\,sc}, t \in T, d \in D \tag{29}$$

$$\overline{AY}_{dgg't} = \overline{AY}_{dgg't} + \overline{Y}_{dgg't} - \overline{Y}_{dgg',t-(\frac{LT^{pipe}}{n})} \quad \forall\{g,g'\} \in N_{gg'}, d \in D, t \in T, g < g' \tag{30}$$

$$\overline{\overline{AY}}_{dgrt} = \overline{\overline{AY}}_{dgr,t-1} + \overline{\overline{Y}}_{dgrt} - \overline{\overline{Y}}_{dgr,t-(\frac{LT^{pipe}}{n})} \quad \forall\{g,r\} \in GR_{gr}, d \in D, t \in T \tag{31}$$

Eqs. (32)–(35) are introduced to avoid the installation of more than one diameter size d for any type of pipelines in each time period.

$$\sum_{d\in D} AY_{dgg't} \le 1 \qquad \forall\{g,g'\} \in N^{pipe}_{gg'}, t \in T, g < g' \tag{32}$$

$$\sum_{d\in D} AY^S_{d\,g\,sc\,t} \le 1 \qquad \forall\{g,sc\} \in GS_{g\,sc}, t \in T \tag{33}$$

$$\sum_{d\in D} \overline{AY}_{dgg't} \le 1 \qquad \forall\{g,g'\} \in N_{gg'}, t \in T, g < g' \tag{34}$$

$$\sum_{d\in D} \overline{\overline{AY}}_{dgrt} \le 1 \qquad \forall\{g,r\} \in GR_{gr}, t \in T \tag{35}$$

3.3.6. CO_2 reservoirs

The reservoir CO_2 inventory for each time period is equal to the inventory of the previous time period and the total flowrates to the reservoir.

$$RI_{rt} = RI_{r,t-1} + n \sum_{g\in GR_{gr}} \sum_{c\in C} \sum_{h\in H} WF_c \cdot \overline{\overline{Q}}_{grtch} \quad \forall r \in R, t \in T, c \in C, h \in H \tag{36}$$

where n is the duration of time periods t.

The inventory level (RI_{rt}) is limited by an upper bound as described in the constraint below.

$$RI_{rt} \le \sum_{d\in D} \sum_{g\in GR_{gr}} cap^R_r \cdot \overline{\overline{AY}}_{dgrt} \qquad \forall r \in R, t \in T \tag{37}$$

where cap^R_r stands for the reservoir capacity.

3.3.7. H_2 imports

The import rate cannot exceed a percentage (ι) of the total hydrogen demand.

$$\sum_{g\in G} Imp_{gtch} \le \iota \sum_{g\in G} TD_{gtch} \qquad \forall t \in T, c \in C, h \in H \tag{38}$$

3.3.8. Electricity production from renewables

Hydrogen produced by water electrolysis (Pr_{pgtch}) is equal to the total electricity generation from renewables ($\widehat{Pr}_{egtch}$) minus the electricity which is curtailed (CL_{gtch}), multiplied by the efficiency factor (η_t) of water electrolysis.

$$Pr_{pgtch} = \eta_t \cdot (\sum_{e\in E} \widehat{Pr}_{egtch} - CL_{gtch}) \quad \forall p \in \{WE\}, g \in G, t \in T, c \in C, h \in H \tag{39}$$

The electricity generation for each renewable type e in each region g, time period t, cluster c and hour h depends on the availability of the renewable e in region g, cluster c and hour h and the renewable capacity (NR_{egt}).

$$\widehat{Pr}_{egtch} = AV_{egch} \cdot NR_{egt} \qquad \forall e \in E, g \in G, t \in T, c \in C, h \in H \tag{40}$$

The renewables capacity in time period t is equal to the new invested capacity in this time period plus the capacity in the previous time period for each renewable type e and region g.

$$NR_{egt} = NR_{eg,t-1} + IR_{egt} \qquad \forall e \in E, g \in G, t \in T \tag{41}$$

The installation of renewables farms is limited by land availability (la_{eg}) as described in Eq. (42).

$$NR_{egt} \le la_{eg} \qquad \forall e \in E, g \in G, t \in T \tag{42}$$

3.3.9. Fuel consumption

Gas consumption (V^{gas}_t) depends on the production rate (Pr_{pgtch}) of reforming technologies which include Steam Methane Reforming and Auto-thermal Reforming and their efficiency (η_{pt}).

$$V^{gas}_t = \sum_{p\in\{SMRCCS,ATRCCS\}} \sum_{g\in G} \sum_{c\in C} \sum_{h\in H} WF_c \cdot \frac{Pr_{pgtch}}{\eta_{pt}} \qquad \forall t \in T \tag{43}$$

Biomass consumption (V^{bio}_{gt}) depends on the production rate of biomass gasification (Pr_{pgtch}) and the efficiency (η_{pt}). Biomass consumption is restricted according to biomass availability ($BA_g t$) in each region.

$$V^{bio}_{gt} = \sum_{p\in\{BGCCS\}} \sum_{c\in C} \sum_{h\in H} WF_c \cdot \frac{Pr_{pgtch}}{\eta_{pt}} \qquad \forall t \in T \tag{44}$$

$$V^{bio}_{gt} \le ba_{gt} \qquad \forall g \in G, t \in T \tag{45}$$

3.3.10. CO_2 emissions

The total CO_2 emissions (E_t) for hydrogen production depend on the production rate (Pr_{pgtch}) according to Eq. (46):

$$E_t = \sum_{p\in P} \sum_{g\in G} \sum_{c\in C} \sum_{h\in H} WF_c \cdot y^e_{pt} \cdot Pr_{pgtch} \qquad \forall t \in T \tag{46}$$

where y^e_{pt} is the emission coefficient for each production technology p. The aforementioned coefficient denotes the quantity of CO_2 emitted per MWh of produced H_2.

An emission target (et_t) for the hydrogen production is considered in the model as defined by Eq. (47).

$$E_t \le et_t \qquad \forall t \in T \tag{47}$$

The model described in this Section comprising of Eqs. (1)–(47), is formulated as an MILP (Mixed Integer Linear Programming) model and it is implemented in GAMS.

4. Hierarchical solution procedures

Due to the high spatio-temporal resolution, the resulting model is computational intensive. Therefore, two solution procedures have been developed to reduce the computational time providing near optimal strategic solutions. The proposed hierarchical approaches are described in Fig. 5.

Hierarchical Approach 1 (HA1) consists of two steps. The first step includes the solution of the model dividing the day in 6 time intervals of 4 h, which decrease the model size significantly. From this step, the production and storage investment decisions (NP_{pgt}, NS_{sgt}) are determined. In the second step, a reduced model with 1-hour daily resolution is solved determining all the remaining decision variables.

The first step of Hierarchical Approach 2 (HA2) includes the model solution without considering the pipeline infrastructure design. Thus, the decision variables ($Y_{dgg't}$, Y^S_{dgst}, $\overline{Y}_{dgg't}$, $\overline{\overline{Y}}_{dgrt}$, $AY_{dgg't}$, AY^S_{dgst}, $\overline{AY}_{dgg't}$, $\overline{\overline{AY}}_{dgrt}$) as well as Eqs. (6)–(7) and (25)–(35) are not taken into account. To ensure the feasibility of the pipeline network, an upper bound, which is equal to the maximum flow, is set for the regional flows. Consequently, Step 1 facilitates the solution of the model as the number of discrete variables decreases reducing the combinatorial complexity. Then, the second step includes the solution of the reduced model in

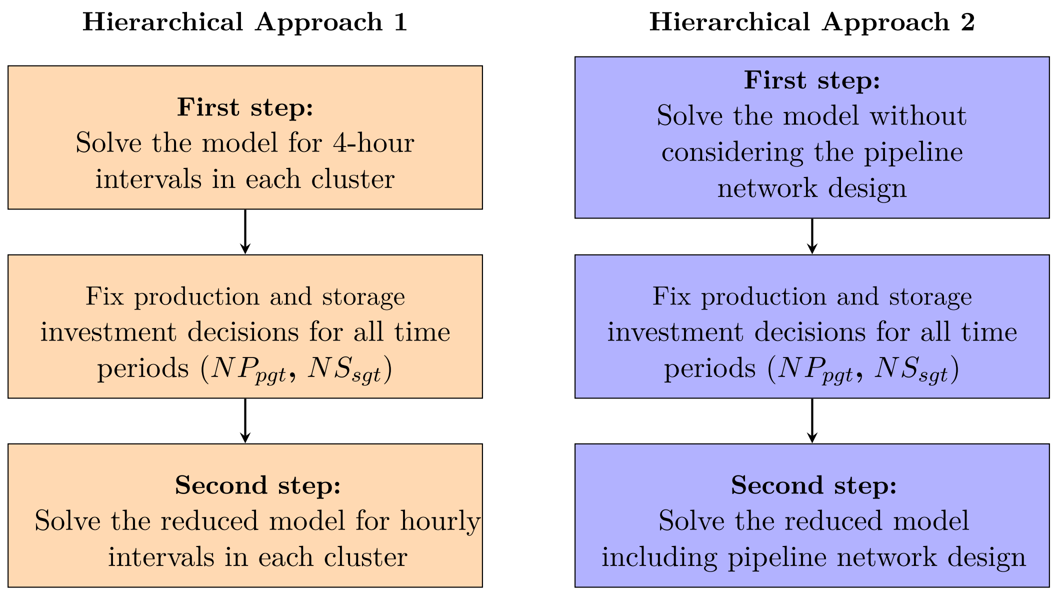

Fig. 5. Hierarchical solution procedures.

which production and storage investment decisions (NP_{pgt}, NS_{sgt}) are fixed from the first step. In the second step, the pipeline infrastructure design and all the other decision variables are defined.

5. Case study

The MILP framework investigates the optimal hydrogen infrastructure for meeting heating hydrogen demand in Great Britain.

5.1. Heat demand

The present work investigates the optimal strategy for hydrogen investments to meet hydrogen residential demand. Hydrogen hourly demand is obtained from gas historical heating consumption data over a number of years in Great Britain (Charitopoulos et al., 2023), which is adjusted to the hydrogen annual demand according to System Transformation scenario from Future Energy Scenarios (National Grid ESO, 2022). Moreover, the demand has spatial variations to provide a more realistic infrastructure planning. For each 5-year time period, one typical year is considered with hourly demand.

5.2. Biomass availability

Biomass gasification is a key technology in hydrogen production as it contributes in the reduction of the net CO_2 emissions of the system. In this study, biomass gasification feedstock includes non-waste biomass consisting of agricultural residues, forestry residues and energy crops. The Climate Change Committee explored the impact of important factors of land use and land management (Abraham et al., 2018). Different scenarios for future UK non-waste biomass production are quantified. For this case-study, high biomass scenario is considered in which 50,000 ha p/a of combined reforestation and afforestation rates are assumed (Abraham et al., 2018). In this scenario, it is estimated that 140 TWh p/a of non-waste biomass will be available by 2050.

The available biomass sources (forestry, agricultural, energy crops) are discretised in the 13 region of Great Britain according to Local gas Distribution Zones (LDZ). It is assumed that there is no biomass transportation between the regions. Thus, the availability of biomass gasification feedstock in each region is estimated using the geographically distributed data analysis according to Calderón et al. (2017). The detailed data can be found in the Supplementary Information.

6. Results & discussion

In this section, the applicability of the proposed optimisation framework is demonstrated through an implementation of the case study in Section 5. On the first part the base case is presented. The second part includes a what-if analysis in different parameters of the model (gas price, carbon tax, biomass availability, interest rate). The MILP model is implemented in GAMS Development Corporation (2023) Version 41.5.0 and solved with (Gurobi Optimization, LLC, 2023) Version 9.5.2 using a machine with 128 GB RAM and CPU 3.00 GHz. Termination criteria are set to 8 h CPU time limit or 5% optimality gap for monolithic optimisation runs. Regarding the optimisation runs for hierarchical approaches, termination criteria are set to 4 h CPU time limit or 2% optimality gap for each step.

6.1. Base case

The optimal production infrastructure to meet hydrogen domestic heating demand in Great Britain is illustrated in Fig. 6. A total of 15 GW are installed in 2035 while BEIS (2021c) has suggested a hydrogen capacity of 7–20 GW by early 2030s. The total capacity is increased to 40.6 GW in 2050. Reforming technologies (SMR CCS and ATR CCS) are mainly established due to their cost efficiency and their reduced CO_2 emissions as they are coupled with carbon capture and storage system. The technology mix in 2050 consists of 7.5 GW of biomass gasification with CCS and 0.1 GW of water electrolysis. The electricity required for water electrolysis is generated from wind onshore farms with capacity of 174 MW in NT.

Storage investments play an important role in hydrogen infrastructure strategy to meet peak demand. In total, hydrogen storage infrastructure of 172 GWh is required in 2050. Pressured storage vessels installed in all GB regions are the most cost efficient option for stored hydrogen.

Hydrogen and CO_2 transmission between regions take place through pipelines. As illustrated in Fig. 6, hydrogen pipeline network is installed from 2035 connecting most of the regions on the west part of GB, while there is no transmission between the regions in Wales. On the other hand, most of the neighbouring CO_2 pipeline connections are allowed. Two reservoirs, one in the northern and one in the southern North Sea, are established for CO_2 storage.

The importance of the hourly resolution can be demonstrated in Fig. 7 as significant demand fluctuations are observed on a daily basis.

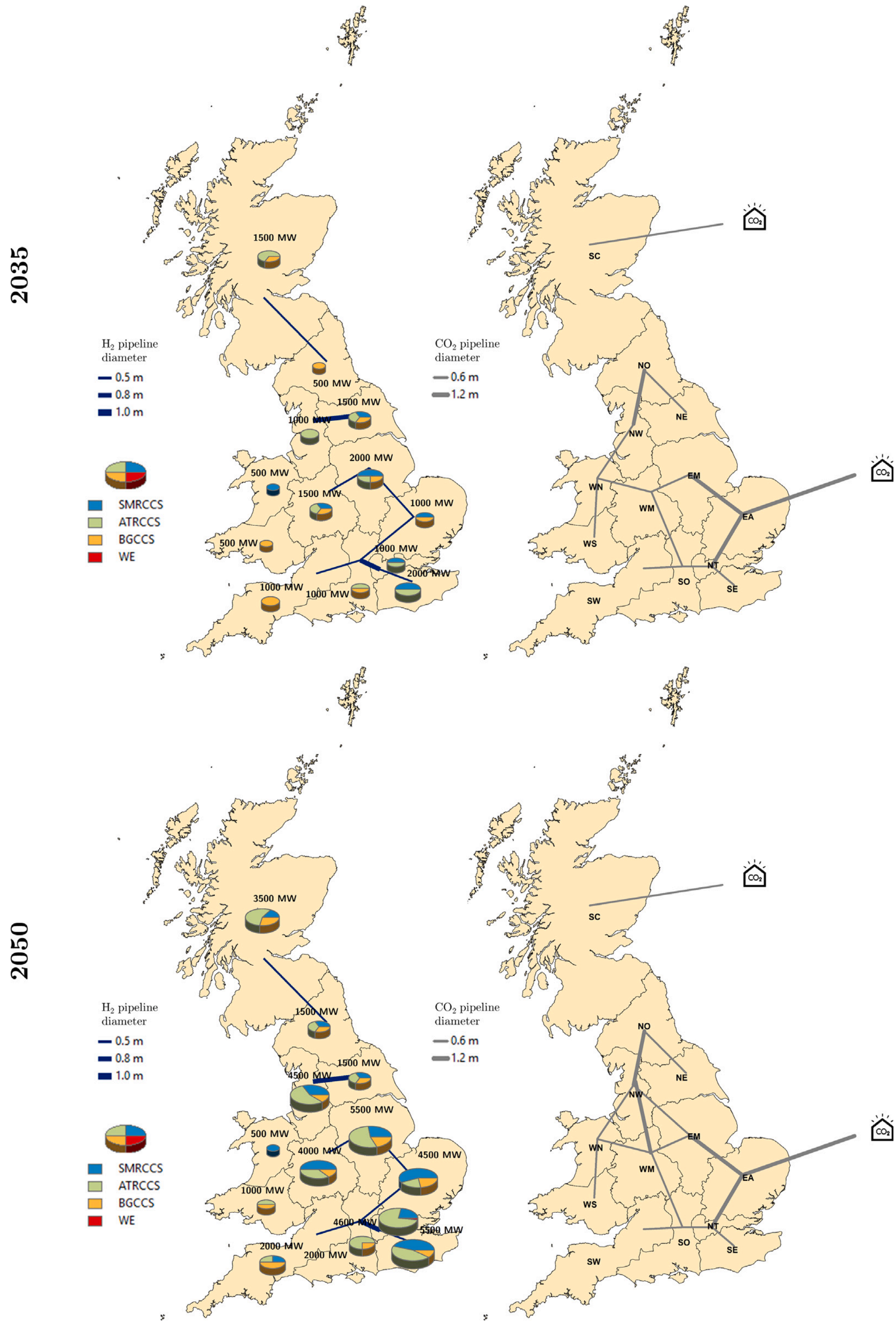

Fig. 6. Production capacity in 2035 and 2050.

Six representative days for each 5-year time step are selected using k-medoids clustering. Each representative day has a different weight factor (WF), which indicates its frequency. Production and storage rates as well as the hourly hydrogen demand are illustrated.

Day 1 constitutes the coldest day of the year, in which 170 GWh of storage and production rate around 30–40 GW are required to meet the peak demand that reaches 65 GW. Day 2 is a typical winter day representing 98 days of the year. In this case, production rate fluctuates from 15–25 GW and storage requirements reach 120 GW. Concerning Day 3, this day represents a cold day of the year with lower hydrogen heat demand and consequently lower production and storage requirements than Day 2.

Days 4–5 are spring/summer days with hydrogen demand less than 15 GW. Regarding these days, production rate and storage requirements

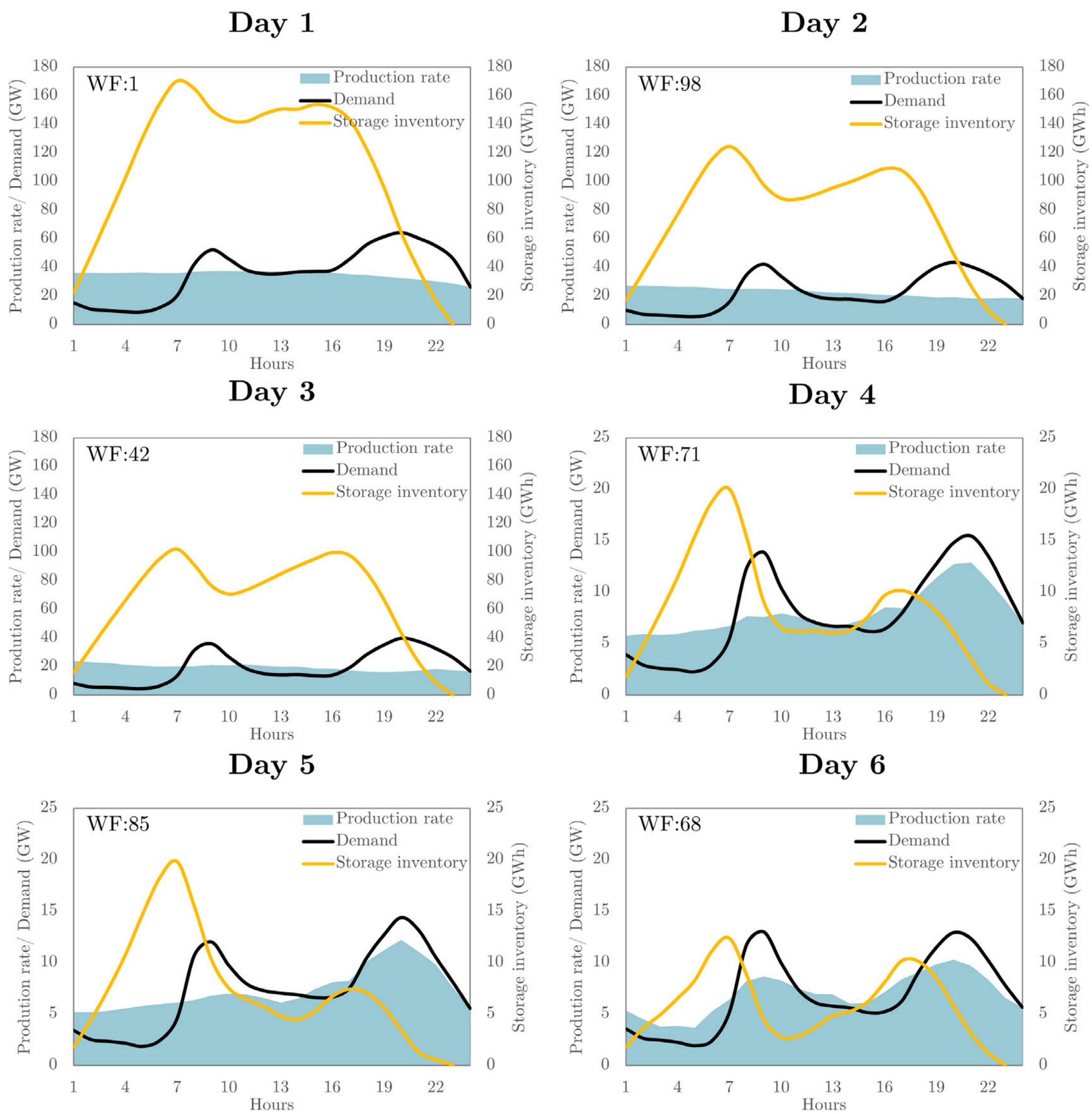

Fig. 7. Total demand, production and storage rate in GB in hourly resolution in 2050.

does not exceed 15 GW and 20 GWh, respectively. Lastly, Day 6 is a representative of summer days accounting for 68 days of the year.

Consequently, hydrogen system adaptability need to be enhanced to meet residential demand fluctuations. To this end, flexible production and storage investments are required to meet the variability of storage needs during a year.

The total cost of building the infrastructure network reaches £b 33.5. The cost breakdown is summarised in Fig. 8. Production capital and operating costs have the greatest contribution in the total system cost. Furthermore, the natural gas and biomass cost, which are used as feedstock for reforming and gasification technologies respectively, have significant effect on the total cost. The levelised cost of hydrogen is estimated 77 £/MWh H_2 without taking account of CO_2 emissions tax. On the other hand, if we consider CO_2 price, hydrogen levelised cost reduces to 56 £/MWh H_2 because of BG with CCS negative CO_2 emissions.

Most of the UK reports do not demonstrate hydrogen levelised cost of the total infrastructure but they focus on hydrogen production levelised cost. UK Department for Business, Energy & Industrial Strategy (BEIS, 2021b) and Energy Networks Association (Ena, 2020) reports hydrogen production levelised costs which vary 40–70 £/MWh H_2 for reforming technologies with CCS, 60–140 £/MWh H_2 for PEM electrolysis and −30–40 £/MWh H_2 for BG with CCS.

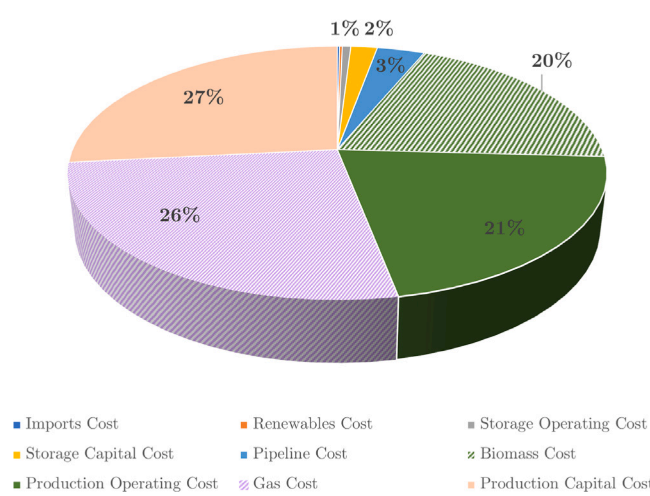

Fig. 8. Cost breakdown.

Table 1
Base case model size and computational performance.

Approach	Monolithic	HA 1		HA 2	
		Step 1	Step 2	Step 1	Step 2
Continuous Variables	163,192	43,472	163,192	163,192	163,192
Discrete Variables	776	776	776	328	776
Equations	270,314	67,274	270,314	223,026	270,314
Computational Time (h)	8	4	2.2	0.4	3.7
Optimality Gap (%)	8.1	4.6	1.9	1.5	1.8
Objective Function Value (£b)	34.2		34.1		33.5

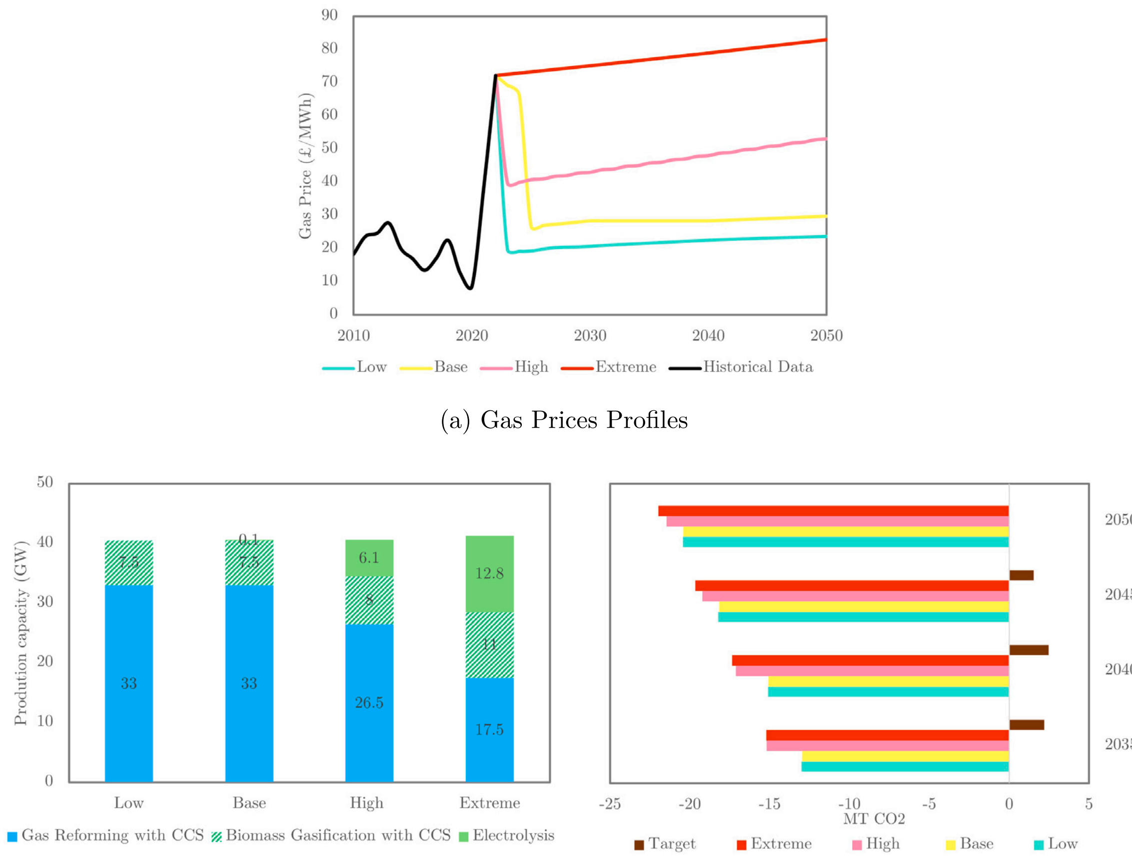

(a) Gas Prices Profiles

(b) Technology Mix

(c) CO_2 Emissions

Fig. 9. Sensitivity analysis for gas price.

In Table 1, model size and computational performance of the base case are summarised, while the importance of the Hierarchical Approaches is illustrated. Regarding model size, fixed variables are included in the total number of variables. As Table 1 depicts, HA 1 results in a slightly better solution than the monolithic run reducing CPU time by 23%. Concerning HA 2, as it is showed on Table 1, it can reduce the computational time by 50% while the objective function is decreased to £b 33.5. Consequently, both of the Hierarchical Approaches can achieve more cost-efficient design decisions using less computational time. The reason behind this is the high combinatorial complexity of the monolithic optimisation run, preventing it from achieving an optimality gap smaller than 8.1%. Thus, these approaches constitute a first step for the model's decomposition which is necessary for the introduction of new features to increase the fidelity.

6.2. What-if analysis

Hydrogen supply chain optimisation is contingent on a multitude of techno-economic parameters. To provide a more realistic strategy and a more holistic view of the problem, a what-if analysis is presented in this Section. More specifically, gas price, carbon tax and biomass availability are studied to investigate their impact on production technology mix and total net CO_2 emissions.

6.2.1. Gas price sensitivity analysis

Hydrogen infrastructure optimisation is strongly dependent on natural gas price as it is the feedstock for reforming technologies. Four different gas price profiles are taken into consideration based on historical data, BEIS (2020) and National Grid ESO (2022) as displayed in Fig. 9(a).

In Fig. 9(b), the technology mix in 2050 is presented. In the low gas price case, reforming and biomass gasification technologies, which are coupled with CCS, are installed. For the base case, in which there is a slight increase in the gas prices, an additional 0.1 GW of WE is installed. On the other hand, in high and extreme cases, WE investments of 6.1 GW and 12.8 GW are commissioned respectively by 2050. Furthermore, biomass gasification capacity increases when gas prices rise. Reforming investments capacity decrease remarkably by 53% comparing extreme to low and base cases.

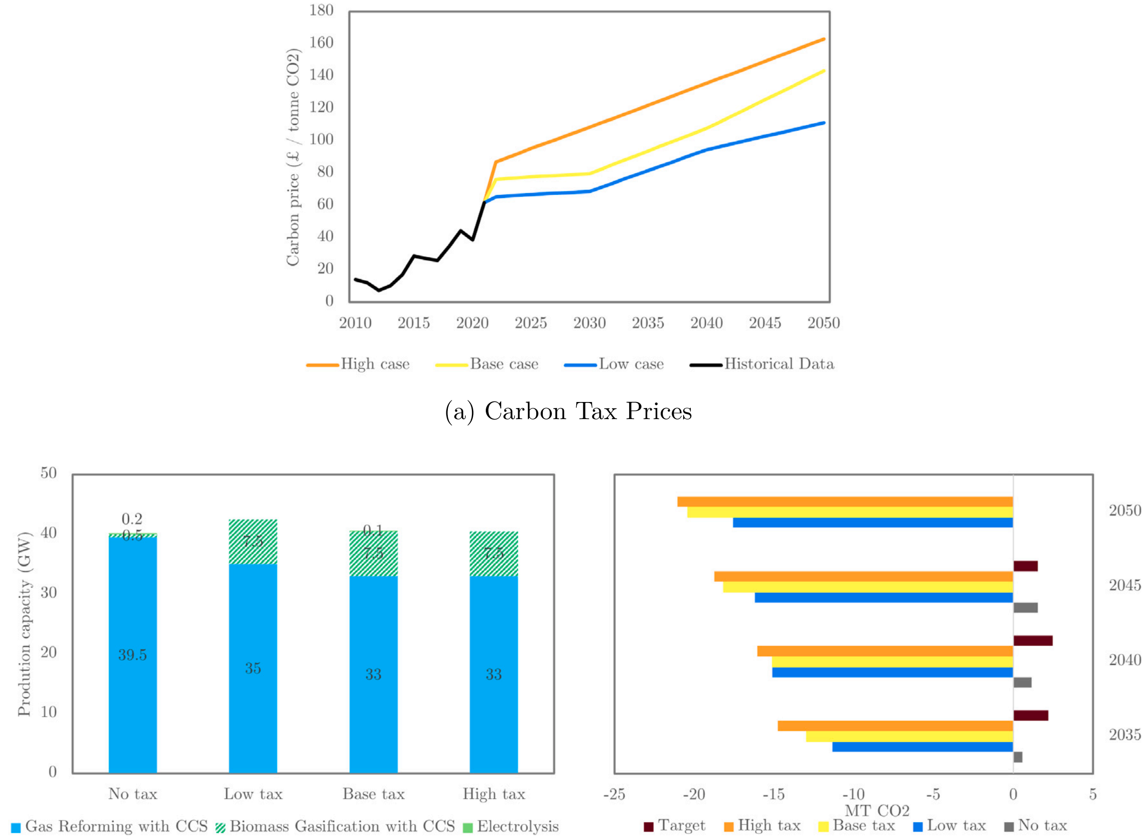

(a) Carbon Tax Prices

(b) Technology Mix

(c) CO_2 Emissions

Fig. 10. Sensitivity analysis for carbon tax.

Furthermore, higher gas prices have a beneficial effect on the carbon footprint of the system due to the lower production capacity in reforming technologies. As illustrated in 9(c), extreme gas price case lead to lower CO_2 net emissions in comparison with the other cases. Although low and base gas price cases have the same production capacity in reforming technologies, it is observed that low gas price case has slightly reduced CO_2 net emissions. This difference can be explained as in low gas price case, there is higher capacity in ATR with CCS which has lower environmental footprint than SMR with CCS.

With regard to the levelised cost, a small decrease is observed in low gas price case (74 £/MWh H_2) in relation with the base case in which levelised cost is equal to 77 £/MWh H_2 without considering carbon tax cost. Nevertheless, levelised cost reaches 88 £/MWh H_2 and 95 £/MWh H_2 in high and extreme gas price cases, respectively.

6.2.2. Carbon tax sensitivity analysis

Carbon price is an essential driver to reduce GHG emissions and achieve Net-Zero target by 2050. In this Section, a sensitivity analysis is conducted to investigate the influence of carbon price in net emissions of the hydrogen system. Three cases (low, base, high) of carbon prices profiles are studied which are obtained from National Grid ESO (2022). CO_2 emissions target is calculated from the total emissions budgets which are established by the UK legislation (CCC, 2020; BEIS, 2021a).

The technology mix for each carbon tax case is illustrated in Fig. 10(b). Implementing a carbon tax policy can increase production capacity in biomass gasification and decrease investments in reforming technologies as the system benefits from negative emissions from biomass gasification.

Fig. 10(c) showcases the significant effect of carbon tax in CO_2 net emissions. If carbon tax policy is not introduced, the total net emissions are positive while they reach zero by 2050 to achieve the net zero emissions goal. On the contrary, negative net emissions are observed from 2035 if carbon tax policy is enforced. Implementing a high tax policy can result in 20% less emissions in 2050 in comparison with the low tax case.

Furthermore, the enforcement of a carbon tax can decrease notably the levelised cost of hydrogen from 65 £/MWh H_2 to 61 £/MWh H_2 for the case of low tax. In the cases of base and high carbon tax policies, hydrogen levelised cost is further reduced to 56 £/MWh H_2 and 54 £/MWh H_2, respectively.

6.2.3. Biomass sensitivity availability analysis

Biomass gasification with CCS is a key technology for achieving Net-Zero goal as it results in negative CO_2 emissions. Consequently, in this study, 3 cases are examined including two cases of 50% (base case) and 30% availability of total biomass as calculated in Section 5.2 and a case that no biomass investments are allowed as shown in Fig. 11(a).

In the case of 30% availability of biomass, reforming technologies are mainly invested (36.5 GW) while only 4 GW of BG with CCS production capacity are installed by 2050 as shown in Fig. 11(b). Concerning the case of 50% availability, there is an increase in the BG capacity to 7.5 GW and a decrease in reforming capacity to 33 GW. Moreover, 0.1 GW of WE are established by 2050. Alternatively, when no biomass is available, a large investment of 35.6 GW in WE is observed and an investment of 21 GW in reforming hydrogen production. In this case, there is an augmentation of 26 GW of total production capacity in 2050. This outcome can be interpreted as green hydrogen from WE is required so that the system can reach Net-Zero emissions target by 2050.

Fig. 11(c) illustrates the net CO_2 emissions of hydrogen production system. When there is more biomass available, there is significant

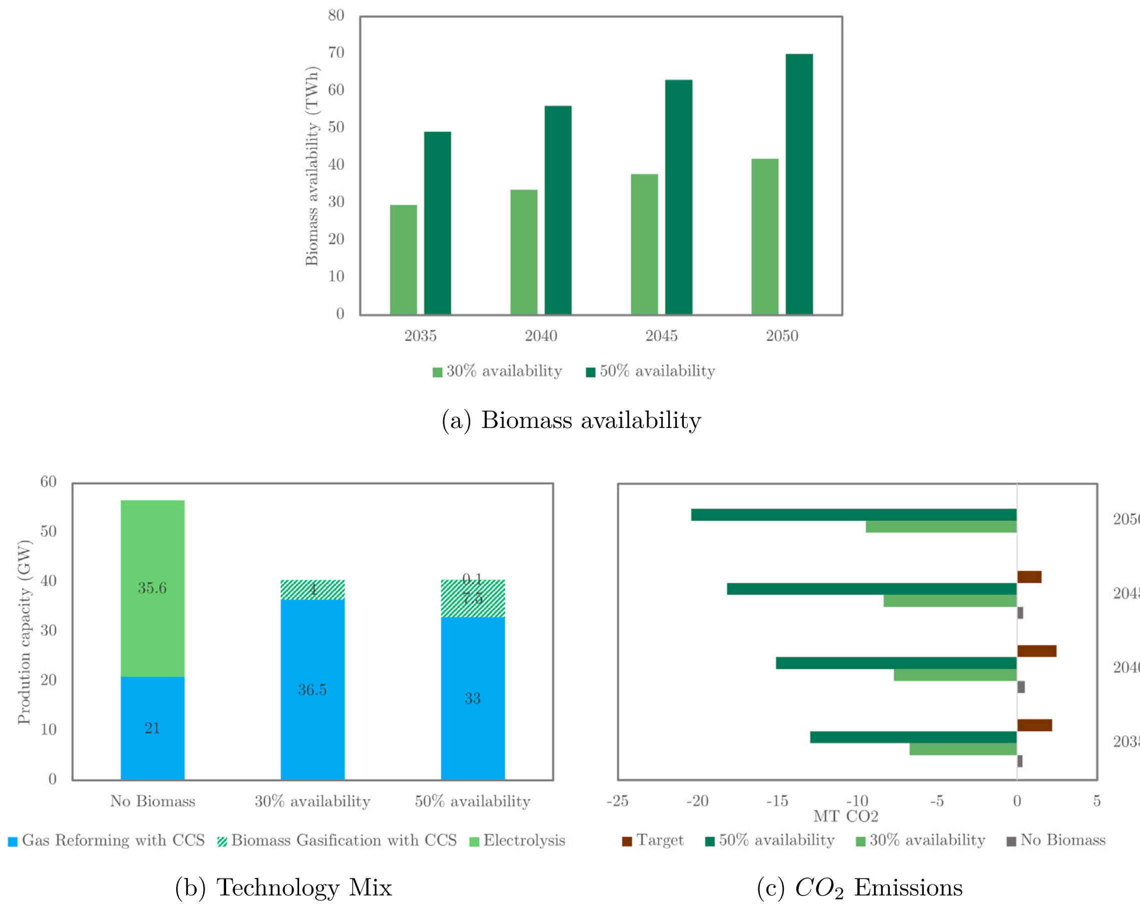

Fig. 11. Sensitivity analysis for biomass availability.

decrease in the total net emissions. On the other hand, when there is no biomass availability, the net emissions are positive for all time period while they reach zero levels in 2050 to achieve Net-Zero goal.

Biomass availability has a great impact on hydrogen levelised cost. In the case that 30% of the biomass is available, an augmentation of hydrogen levelised cost is observed from 56 £/MWh H_2 to 63 £/MWh H_2 due to higher CO_2 emissions from the system. Moreover, non-deployment of biomass gasification result in an increase of the levelised cost to 100 £/MWh H_2 due to the significant rise in WE investments. WE is the least cost effective hydrogen production technology as it not mature enough for widespread use at this time. However, investments in WE are required to reach carbon emission targets in the event that biomass availability is zero.

7. Concluding remarks

In this study, an optimisation-based framework is developed to facilitate the investigation of design and operating decisions in hydrogen infrastructure in the UK for the transition to a low-carbon energy economy. Insights for policy making can be obtained for a hydrogen strategy over the next decades. This work also focuses on two hierarchical solution procedures to tackle with the combinatorial complexity of the resulting model. These approaches can deal efficiently the large-scale optimisation problem and enable greater model complexity as they can provide improved solutions and reduce computational time up to 50%.

The MILP model considers hydrogen production, storage and transmission as well as captured CO_2 transmission and storage. Reforming technologies with CCS are the most cost-effective low-carbon alternative options for hydrogen production. The deployment of gas technologies with CCS and biomass gasification with CCS leads to a low-emissions infrastructure strategy. However, production investment decisions are highly dependent on gas prices. Optimal design includes notably increased capacity in WE when higher gas prices are considered. Regarding hydrogen transmission, it is based on a pipeline network which connects most neighbouring regions in GB. Furthermore, a CO_2 pipeline network and two CO_2 reservoirs are essential to support the CCS system to achieve lower CO_2 emissions. With regard to storage infrastructure, the system requires 172 GWh of hydrogen storage to meet demand variability.

Future research focuses on the introduction of uncertainty in hydrogen supply chain model for a more risk averse infrastructure strategy. In addition, the effects of economies-of-scale and learning rate in infrastructure design decisions will be studied. Moreover, sector coupling of heat and power sector will be considered to present a more holistic approach for heat decarbonisation future decisions. In parallel, the exploration of new decomposition techniques and solution approaches will be investigated to tackle with the combinatorial complexity and high computational times.

Declaration of competing interest

The authors declare that they have no known competing financial interests or personal relationships that could have appeared to influence the work reported in this paper.

Acknowledgement

Authors gratefully acknowledge the financial support from Engineering and Physical Sciences Research Council (EPSRC), United Kingdom under the project EP/T022930/1.

Notation

Acronyms and abbreviations

ATR	Auto-Thermal Reforming
BG	Biomass Gasification
CCS	Carbon Capture and Storage
GHG	Greenhouse Gas
HA	Hierarchical Approach
MILP	Mixed-Integer Linear Programming
PEM	Polymer electrolyte membrane
SC	Supply Chain
SMR	Steam Methane Reforming
WE	Water Electrolysis

Indices

c	cluster
d	diameter size
e	renewable technology
h	hours
g	region
p	production technology
r	reservoir
s	storage technology
t	time period

Sets

C	set of clusters c
D	set of diameter sizes d
E	set of renewable technologies e
H	set of hours h
G	set of regions g
N	set of neighbouring regions g and g'
N^{pipe}	set of pipeline connections between region g and g'
P	set of production technologies p
R	set of reservoirs r
S	set of storage technologies s
T	set of time periods t
SC	set of storage vessels s
SV	set of storage caverns s
GI	set of regions g in which international import can take place
GR	set of collection points g and reservoir r connections
GS	set of regions g in which storage caverns sc are located

Parameters

δ	ratio of hydrogen regional pipeline operating costs to capital costs (%)
$\overline{\delta}$	ratio of CO_2 regional pipeline operating costs to capital costs (%)
$\overline{\overline{\delta}}$	ratio of CO_2 regional pipeline operating costs to capital costs (%)
η_{pt}	efficiency of production technology p of each time period t (MW H_2 / MWe)
ι	maximum percentage of international hydrogen imports over the total demand (%)
AV_{egch}	availability of renewable technology e in region g, cluster c and hour h (%)
ba_{gt}	biomass availability in time period t and region g (MWh)
cap_p^P	unit capacity for production type p (MW/unit)
cap_p^{Pmax}	maximum capacity of a hydrogen production plant of type p (MW/unit)
cap_p^{Pmin}	minimum capacity of a hydrogen production plant of type p (MW/unit)
cap_r^R	total capacity of reservoir r (kg CO_2)
cap_s^S	unit capacity for storage type s (MW/unit)
cap_s^{Smax}	maximum capacity of a storage facility of type s (MWh/unit)
cap_s^{Smin}	minimum capacity of a storage facility of type s (MWh/unit)
CO_2	pipeline of diameter size d (£/km)
c_t^{bio}	cost of biomass in time period t (£/MWh)
c_t^{gas}	cost of gas in time period t (£/MWh)
crf	capital recovery factor
ct_t	carbon tax in time period t (£/kg CO_2)
dfc_t	discount factor for capital costs in time period t
dfo_t	discount factor for operating costs in time period t
$D_{gg'}^{Pipe}$	delivery distance of a pipeline between regions g and g' (km)
D_{gr}^{Res}	distance from CO_2 collection point in region g to reservoir r (km)
$D_{gg'}^{Road}$	delivery road distance of hydrogen between regions g and g' (km)
$D_{g\,sc}^{St}$	distance between region g and storage cavern sc
dr	discount rate (%)
et_t	CO_2 emissions target for time period t ($MtCO_2$)
la_{eg}	land availability for renewables technology e and region g (MW)
LT^{on}	lifetime of onshore CO_2 pipeline
LT^{off}	lifetime of offshore CO_2 pipeline
LT^{pipe}	lifetime of hydrogen pipeline
LT_p^P	lifetime of production technology p
LT_s^S	lifetime of storage technology s
n	duration of time periods (y)
nel	economic life cycle of capital investments (y)
p^{imp}	price of hydrogen import (£/MWh)
pc_d	capital costs of a hydrogen pipeline of diameter size d (£/km)
$\overline{pc}_d$	capital costs of an onshore CO_2 pipeline of diameter size d (£/km)
$\overline{\overline{pc}}_d$	capital costs of an offshore CO_2 pipeline of diameter size d (£/km)
pcc_{pt}	capital cost of a production plant of type p (£/MW)
poc_{pt}^F	fixed operating production cost in a production plant of type p (£/MW/y)
poc_{pt}^V	variable operating production cost in a production plant of type p (£/MW)
q_d^{Hmax}	maximum flowrate in a hydrogen pipeline of diameter size d (MW/h)
q_d^{Cmax}	maximum flowrate in a CO_2 pipeline of diameter size d (kg CO_2/h)
Q_s^{Imax}	maximum injection rate for each storage type s (MW/h)
Q_s^{Rmax}	maximum retrieval rate for each storage type s (MW/h)
rc_{et}	capital cost of renewable technology e in time period t (£/MW)
RD_p	maximum ramp down for production technology p (%)
ReC	renewables operating cost (£)
ro_{et}	operating cost of renewable technology e in time period t (£/MW/y)

RU_p	maximum ramp up for production technology p (%)
scc_s	capital cost of a storage facility of type s (£/MW H_2)
soc_s^F	fixed operating storage cost in a production plant of type p (£/MW H_2/y)
soc_s^V	variable operating storage cost in a production plant of type p (£/MWh)
TD_{gtch}	total hydrogen demand in region g, time period t, cluster c and hour h (MW)
WF_c	weight of cluster c (d)
y_{pt}^c	coefficient of CO_2 capture for production technology p in time period t (kg CO_2/MWh H_2)
y_{pt}^e	coefficient of CO_2 emissions for production technology p in time period t (kg CO_2/MWh H_2)

Integer Variables

IP_{pgt}	number of investments of the new production technologies p in region g in time period t (units)
IS_{sgt}	number of investments of new storage facilities of type s in region g in time period t (units)
NP_{pgt}	number of available production technologies p in region g in time period t (units)
NS_{sgt}	number of available storage facilities of type s in region g in time period t (units)

Binary Variables

$AY_{dgg't}$	availability of hydrogen pipeline of diameter size d between regions g and g' in time period t
AY_{dgst}^S	availability of hydrogen pipeline of diameter size d between region g and storage cavern s in time period t
$\overline{AY}_{dgg't}$	availability of onshore CO_2 pipeline of diameter size d between regions g and g' in time period t
$\overline{\overline{AY}}_{dgrt}$	availability of offshore CO_2 pipeline of diameter size d between region g and reservoir r in time period t
$Y_{dgg't}$	establishment of hydrogen pipeline of diameter size d between regions g and g' in time period t
Y_{dgst}^S	establishment of hydrogen pipelines of diameter size d between region g and storage cavern s in time period t
$\overline{Y}_{dgg't}$	establishment of onshore CO_2 pipeline of diameter size d between regions g and g' in time period t
$\overline{\overline{Y}}_{dgrt}$	establishment of offshore CO_2 pipeline of diameter size d between region g and reservoir r in time period t

Continuous Variables

BG	biomass cost (£)
CEC	carbon emissions cost (£)
CL_{gtch}	curtailment in region g, time period t, cluster c, hour h (MW)
E_t	total CO_2 emissions in time period t ($MtCO_2$)
FC	fuel cost for regional transport (£)
GC	general Cost for regional transport (£)
IIC	international import cost (£)
Imp_{gtch}	flow rate of international import in region g in time period t (MW)
IR_{egt}	new invested capacity of renewable technology e in region g and time period t (MW)
LC	labour cost for regional transport (£)
MC	maintenance cost for regional transport (£)
NGC	natural gas cost (£)
NR_{egt}	available capacity of renewable e in region g and time period t (MW)
PCC	production capital cost (£)
$PLCC$	pipeline capital cost (£)
$PLOC$	pipeline operating cost (£)
POC	production operating cost (£)
Pr_{pgtch}	production rate of production technology p in region g in time period t (MW)
$\widehat{Pr}_{egtch}$	electricity production from renewable technology e in region g, time period t, cluster c and hour h (MW)
$Q_{gg'tch}$	flowrate of H_2 in region g in time period t (MW)
Q_{gstch}^I	flowrate of H_2 via pipeline from region g to storage type s in time period t, cluster c and hour h (MW)
Q_{sgtch}^R	flowrate of H_2 via pipeline from storage type s to region g in time period t, cluster c and hour h (MW)
$\overline{Q}_{gg'tch}$	flowrate of CO_2 via onshore pipelines between regions g and g' in time period t, cluster c and hour h (kg CO_2/h)
$\overline{\overline{Q}}_{grtch}$	flowrate of CO_2 via offshore pipelines from a collection point in region g to a reservoir r in time period t, cluster c and hour h (kg CO_2/h)
RI_{rt}	inventory of CO_2 in reservoir r in time period t (kg CO_2)
SCC	storage capital cost (£)
SOC	storage operating cost (£)
St_{sgtch}	storage inventory of product type i stored in a storage facility of type s in region g in time period t, cluster c and hour h (MWh)
V_{gt}^{bio}	consumption of biomass in time period t and region g (MWh)
V_t^{gas}	consumption of natural gas in time period t and region g (MWh)

Appendix A. Supplementary data

Supplementary material related to this article can be found online at https://doi.org/10.1016/j.cherd.2024.02.028.

References

Abraham, S., Andrew, T., Bellamy, O., Davies, E., Goater, A., Hay, R., Hemsley, M., Livermore, S., Mackenzie, C., Millar, R., Scudo, A., Smith, S., Thillainathan, I., Wettingfeld, T., Wyatt, N., Barrett, J., Brown, K., Freeman, B., Harry, S.J., Kmietowicz, E., Cornelius, S., Donnison, I., House, J., Murphy, R., Smith, P., Taylor, G., Tubby, I., Willis, K., Whitaker, J., Woods, J., 2018. Biomass in a low-carbon economy. URL www.theccc.org.uk/publications.

Agnolucci, P., Akgul, O., McDowall, W., Papageorgiou, L.G., 2013. The importance of economies of scale, transport costs and demand patterns in optimising hydrogen fuelling infrastructure: An exploration with SHIPMod (Spatial hydrogen infrastructure planning model). Int. J. Hydrog. Energy 38, 11189–11201. http://dx.doi.org/10.1016/j.ijhydene.2013.06.071.

Almansoori, A., Shah, N., 2006. Design and operation of a future hydrogen supply chain: Snapshot model. Chem. Eng. Res. Des. 84, 423–438. http://dx.doi.org/10.1205/CHERD.05193.

Almansoori, A., Shah, N., 2009. Design and operation of a future hydrogen supply chain: Multi-period model. Int. J. Hydrog. Energy 34, 7883–7897. http://dx.doi.org/10.1016/J.IJHYDENE.2009.07.109.

Almaraz, S.D.-L., Azzaro-Pantel, C., Montastruc, L., Domenech, S., 2014. Hydrogen supply chain optimization for deployment scenarios in the Midi-Pyrénées region, France. Int. J. Hydrog. Energy 39, 11831–11845. http://dx.doi.org/10.1016/J.IJHYDENE.2014.05.165.

Almaraz, S.D.-L., Azzaro-Pantel, C., Montastruc, L., Pibouleau, L., Senties, O.B., 2013. Assessment of mono and multi-objective optimization to design a hydrogen supply chain. Int. J. Hydrog. Energy 38, 14121–14145. http://dx.doi.org/10.1016/J.IJHYDENE.2013.07.059.

Almaraz, S.D.-L., Rácz, V., Azzaro-Pantel, C., Szántó, Z.O., 2022. Multiobjective and social cost-benefit optimisation for a sustainable hydrogen supply chain: Application to Hungary. Appl. Energy 325, 119882. http://dx.doi.org/10.1016/J.APENERGY.2022.119882.

BEIS, 2018. Clean growth - transforming heating - overview of current evidence. URL https://assets.publishing.service.gov.uk/government/uploads/system/uploads/attachment_data/file/766109/decarbonising-heating.pdf.

BEIS, 2020. BEIS 2019 fossil fuel price assumptions. URL https://assets.publishing.service.gov.uk/government/uploads/system/uploads/attachment_data/file/863717/beis-2019-fossil-fuel-price-assumptions.pdf.

BEIS, 2021a. Energy consumption in the UK. URL https://www.gov.uk/government/statistics/energy-consumption-in-the-uk-2021.

BEIS, 2021b. Hydrogen production costs 2021. URL https://assets.publishing.service.gov.uk/government/uploads/system/uploads/attachment_data/file/1011506/Hydrogen_Production_Costs_2021.pdf.

BEIS, 2021c. UK hydrogen strategy. URL www.gov.uk/government/publications/uk-hydrogen-strategy.

BEIS, 2022. Progress in reducing emissions 2022 Report to Parliament. URL https://www.theccc.org.uk/publication/2022-progress-report-to-parliament.

BEIS, 2023. 2021 UK greenhouse gas emissions, final figures. URL https://assets.publishing.service.gov.uk/government/uploads/system/uploads/attachment_data/file/1134664/greenhouse-gas-emissions-statistical-release-2021.pdf.

Calderón, A.J., Agnolucci, P., Papageorgiou, L.G., 2017. An optimisation framework for the strategic design of synthetic natural gas (BioSNG) supply chains. Appl. Energy 187, 929–955. http://dx.doi.org/10.1016/J.APENERGY.2016.10.074.

CCC, 2020. Policies for the sixth carbon budget and net zero. URL https://www.theccc.org.uk/wp-content/uploads/2020/12/Policies-for-the-Sixth-Carbon-Budget-and-Net-Zero.pdf.

Charitopoulos, V.M., Fajardy, M., Chyong, C.K., Reiner, D.M., 2023. The impact of 100% electrification of domestic heat in great britain. iScience 26, 108239. http://dx.doi.org/10.1016/J.ISCI.2023.108239.

Element Energy and E4tech, 2018. Cost analysis of future heat infrastructure options. URL https://nic.org.uk/app/uploads/Element-Energy-and-E4techCost-analysis-of-future-heat-infrastructure-Final.pdf.

Ena, 2020. Gas goes green: Hydrogen cost to customer. URL https://www.energynetworks.org/industry-hub/resource-library/gas-goes-green-hydrogen-cost-to-customer-report.pdf.

GAMS Development Corporation, 2023. General algebraic modeling system. https://www.gams.com.

Guillén-Gosálbez, G., Mele, F.D., Grossmann, I.E., 2010. A bi-criterion optimization approach for the design and planning of hydrogen supply chains for vehicle use. AICHE J. 56, 650–667. http://dx.doi.org/10.1002/AIC.12024.

Gurobi Optimization, LLC, 2023. Gurobi Optimizer. Gurobi Optimization, LLC, Houston, TX, URL https://www.gurobi.com.

He, G., Mallapragada, D.S., Bose, A., Heuberger, C.F., Gencer, E., 2021. Hydrogen supply chain planning with flexible transmission and storage scheduling. IEEE Trans. Sustain. Energy 12, 1730–1740. http://dx.doi.org/10.1109/TSTE.2021.3064015.

HM Government, 2021. Net zero strategy: Build back greener. URL https://www.gov.uk/government/publications/net-zero-strategy.

Hugo, A., Rutter, P., Pistikopoulos, S., Amorelli, A., Zoia, G., 2005. Hydrogen infrastructure strategic planning using multi-objective optimization. Int. J. Hydrog. Energy 30, 1523–1534. http://dx.doi.org/10.1016/j.ijhydene.2005.04.017.

Hy4Heat, BEIS, 2021. Safety assessment: Conclusions report (incorporating quantitative risk assessment). URL https://static1.squarespace.com/static/5b8eae345cfd799896a803f4/t/60e399b094b0d322fb0dadc4/1625528759977/conclusions+inc+QRA.pdf.

IEA, 2021. Net zero by 2050 - a roadmap for the global energy sector. URL www.iea.org/t&c/.

Kazi, M.-K., Eljack, F., 2022. Practicality of green H2 economy for industry and maritime sector decarbonization through multiobjective optimization and RNN-LSTM model analysis. Ind. Eng. Chem. Res. 61, 6173–6189. http://dx.doi.org/10.1021/acs.iecr.2c00757, URL https://pubs.acs.org/doi/10.1021/acs.iecr.2c00757.

Kotzur, L., Markewitz, P., Robinius, M., Stolten, D., 2018. Impact of different time series aggregation methods on optimal energy system design. Renew. Energy 117, 474–487. http://dx.doi.org/10.1016/j.renene.2017.10.017, URL https://linkinghub.elsevier.com/retrieve/pii/S0960148117309783.

Kumar, S.S., Lim, H., 2022. An overview of water electrolysis technologies for green hydrogen production. Energy Rep. 8, 13793–13813. http://dx.doi.org/10.1016/j.egyr.2022.10.127, URL http://creativecommons.org/licenses/by/4.0/.

Liang, Z., Rongwong, W., Liu, H., Fu, K., Gao, H., Cao, F., Zhang, R., Sema, T., Henni, A., Sumon, K., Nath, D., Gelowitz, D., Srisang, W., Saiwan, C., Benamor, A., Al-Marri, M., Shi, H., Supap, T., Chan, C., Zhou, Q., Abu-Zahra, M., Wilson, M., Olson, W., Idem, R., Tontiwachwuthikul, P., 2015. Recent progress and new developments in post-combustion carbon-capture technology with amine based solvents keywords: Recent development of PCC process Design and modeling Solvent development Post Build Operations Solvent chemistry Solvent management Mass transfer with reaction. Int. J. Greenh. Gas Control. 40, 26–54. http://dx.doi.org/10.1016/j.ijggc.2015.06.017.

Moreno-Benito, M., Agnolucci, P., Papageorgiou, L.G., 2017. Towards a sustainable hydrogen economy: Optimisation-based framework for hydrogen infrastructure development. Comput. Chem. Eng. 102, 110–127. http://dx.doi.org/10.1016/j.compchemeng.2016.08.005.

National Grid ESO, 2022. Future energy scenarios. URL www.nationalgrideso.com/future-energy/future-energy-scenarios.

Ogumerem, G.S., Kim, C., Kesisoglou, I., Diangelakis, N.A., Pistikopoulos, E.N., 2018. A multi-objective optimization for the design and operation of a hydrogen network for transportation fuel. Chem. Eng. Res. Des. 131, 279–292. http://dx.doi.org/10.1016/J.CHERD.2017.12.032.

Samsatli, S., Samsatli, N.J., 2019. The role of renewable hydrogen and inter-seasonal storage in decarbonising heat – Comprehensive optimisation of future renewable energy value chains. Appl. Energy 233–234, 854–893. http://dx.doi.org/10.1016/j.apenergy.2018.09.159.

Samsatli, S., Staffell, I., Samsatli, N.J., 2016. Optimal design and operation of integrated wind-hydrogen-electricity networks for decarbonising the domestic transport sector in Great Britain. Int. J. Hydrog. Energy 41, 447–475. http://dx.doi.org/10.1016/J.IJHYDENE.2015.10.032.

Seo, S.K., Yun, D.Y., Lee, C.J., 2020. Design and optimization of a hydrogen supply chain using a centralized storage model. Appl. Energy 262, 114452. http://dx.doi.org/10.1016/J.APENERGY.2019.114452.

Sunny, N., Dowell, N.M., Shah, N., 2020. What is needed to deliver carbon-neutral heat using hydrogen and CCS? Energy Environ. Sci. 13, 4204–4224. http://dx.doi.org/10.1039/d0ee02016h.

Walker, I., Madden, B., Tahir, F., 2018. Hydrogen Supply Chain Evidence Base. Department for Business, Energy & Industrial Strategy, URL https://www.gov.uk/government/publications/hydrogen-supply-chain-evidence-base.

Weber, A.C., Papageorgiou, L.G., 2018. Design of hydrogen transmission pipeline networks with hydraulics. Chem. Eng. Res. Des. 131, 266–278. http://dx.doi.org/10.1016/J.CHERD.2018.01.022.